

Development of Skyrmion Brownian Devices*

Ryo ISHIKAWA^{*1}, Minori GOTO^{*2}, Hikaru NOMURA^{*2} and Yoshishige SUZUKI^{*2}

^{*1}Research Laboratory for Future Technology, Research & Development HQ, ULVAC, Inc., 2-1 Yamadaoka, Suita, Osaka 565-0871, Japan

^{*2}Graduate School of Engineering Science, The University of Osaka, 1-3 Machikaneyama, Toyonaka, Osaka 560-8531, Japan

Magnetic skyrmions are vortex-like spin textures that are stabilized due to topological protection and exhibit Brownian motion in solids. Owing to the high applicability of skyrmions in Brownian motion as an information carrier, applications in unconventional computing such as probabilistic and Brownian computing are expected. Some work on how to control the Brownian motion of skyrmions is introduced in this manuscript.

1. Introduction

Although a smart society—which is advancing through technologies such as IoT and 5G—is expected to become the foundation of a sustainable society, there are concerns about increased power demand for computers. To overcome these challenges, it will be necessary to develop innovations that make computers faster, smaller and more energy efficient. Spintronics is one field of research that aims to realize such innovations. Although modern electronic devices use the charge of electrons to store and transport information, the use of electron spin as information carrier is expected to enhance device performance, and various studies are being conducted in the field of spintronics. One subject of research on information carriers in new spin-based devices are magnetic skyrmions (hereafter referred to as “skyrmions”). Skyrmions are topologically protected vortex-like magnetic structures^{1,2} whose motion is enabled by the propagation of spin order in a solid. Applied research on the use of skyrmions has been conducted internationally. Examples of how skyrmions can be used as information carriers include racetrack memory³ and logic devices⁴. In these applications, electric current is used to drive skyrmions in order to transport the skyrmions and process information. In contrast, the use of heat-induced skyrmion transport has also been proposed. Skyrmions are known to exhibit Brownian motion due to ambient heat^{5,6}. Using this property,

their use is anticipated for applications in ultra-low-power computing and probabilistic computing that utilizes fluctuating states. Our research group is developing methods to control skyrmions in pursuit of new-principle computing using skyrmions that exhibit Brownian motion. Until now, the control of skyrmions has primarily been achieved using electric current. However, this approach is unsuitable for achieving ultimate energy efficiency as it is accompanied by Joule heat dissipation. In this study, we attempted to use voltage to control skyrmions. This manuscript introduces recent major achievements including the use of voltage to control skyrmions.

2. Representing information using skyrmions

Before introducing methods of controlling skyrmions, we will first explain how information is represented using skyrmions. Representing information using skyrmions involves defining states based on the presence or absence of a skyrmion, as illustrated in Fig. 1 (a), as well as representing information using the position or arrangement of skyrmions, as illustrated in Fig. 1 (b) and (c). In particular, the latter is an important method of information representation for applications in next-generation computing, as it allows for state changes driven by the Brownian motion of skyrmions.

3. Fabricating magnetic multilayers exhibiting Brownian motion

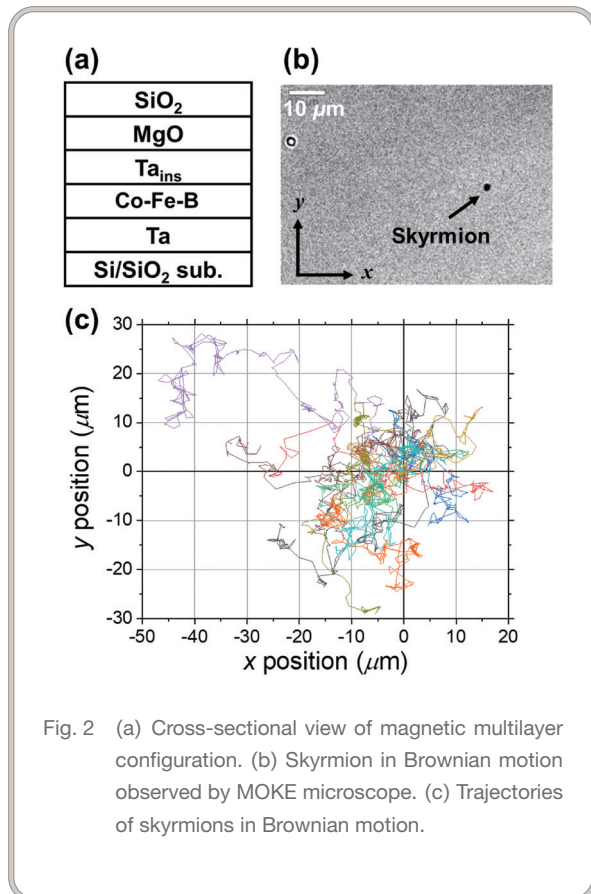
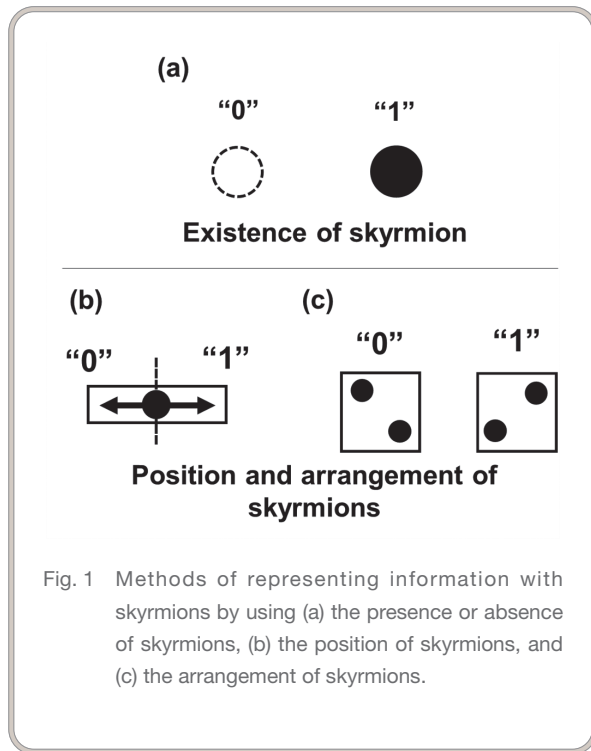
Magnetic multilayers on which skyrmions appear were deposited at room temperature using magnetron sputtering. The multilayer structure is shown in Fig. 2 (a). The perpendicular magnetic anisotropy was controlled by adjusting the thickness of the Ta layer inserted between the Co-Fe-B and MgO layers on a sub-nanometer scale, resulting in samples in which skyrmions appear within the desired temperature range. Fig. 2 (b) shows the

*Presented in Appl. Phys. Lett. 117, 082402 (2020); Appl. Phys. Lett. 119, 072402 (2021); Appl. Phys. Lett. 121, 252402 (2022); and the Journal of the Magnetism Society of Japan, Magnetism, 18 (5), (2023).

^{*1} Research Laboratory for Future Technology, Research & Development HQ, ULVAC, Inc.
(2-1 Yamadaoka, Suita, Osaka 565-0871, Japan)

^{*2} Graduate School of Engineering Science, The University of Osaka
(1-3 Machikaneyama, Toyonaka, Osaka 560-8531, Japan)

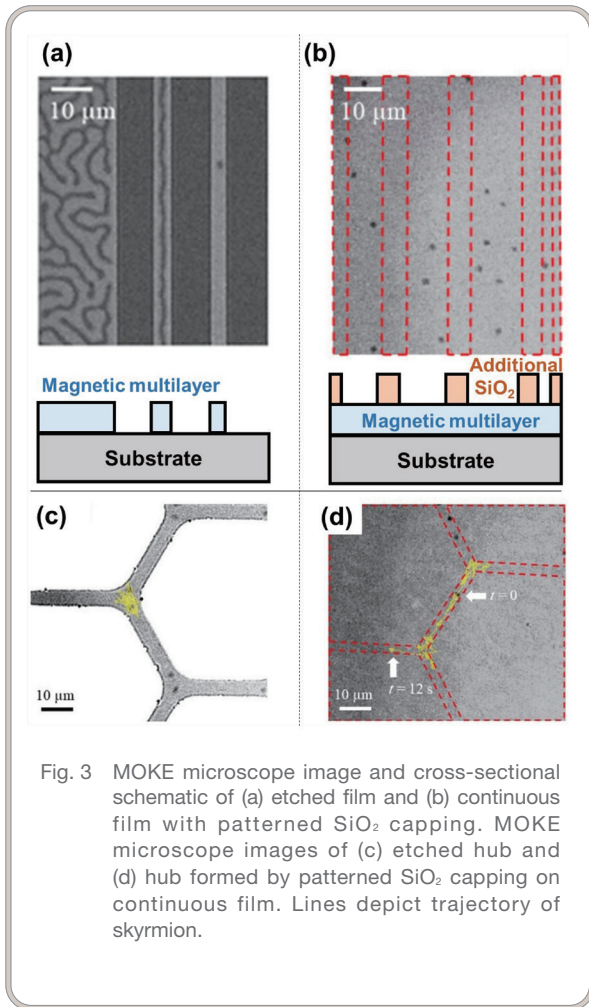
magnetic structure observed by a Magneto Optical Kerr Effect (MOKE) microscope while applying an external magnetic field perpendicular to the stacking direction of the magnetic multilayer.



The black dots of 1 to 2 μm in size are skyrmions. These skyrmions exhibit Brownian motion, and the trajectory of their Brownian motion is shown in Fig. 2 (c). The diffusion coefficient indicating the activity of the Brownian motion of skyrmions was about 10 μm²/s. This value is larger than that of other research groups^{5, 7)}. This is thought to be due to the fact that the magnetic layer deposited at room temperature was amorphous with little pinning.

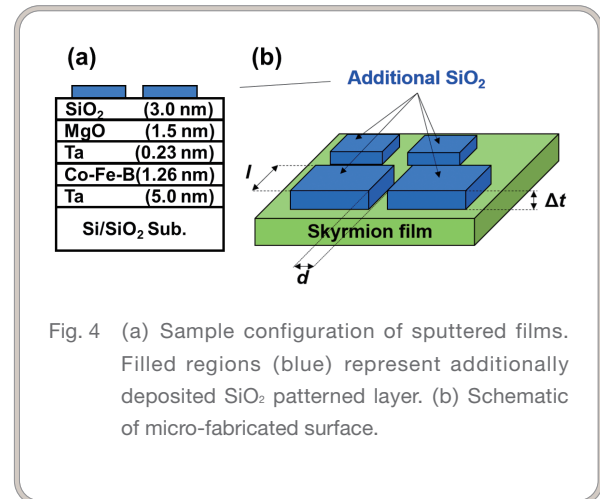
4. Forming skyrmion circuits

Fabricating devices using skyrmions in Brownian motion as information carriers requires circuits that are capable of generating and transporting skyrmions as desired. Jibiki et al.⁸⁾ fabricated skyrmion circuits using two methods: one involving etching a magnetic multilayer into a wire shape to form a circuit, and the other involving the partial formation of an SiO₂ capping layer on a continuous magnetic multilayer film. They then compared the Brownian motion of the skyrmions in each configuration. Fig. 3 (a) shows a skyrmion circuit fabricated by etching the magnetic multilayer film into a wire shape. Circuits called “skyrmion channels,” through which skyrmions can pass, can be created by forming wires. However, the magnetic wire method was found to be problematic due to issues such as the loss of skyrmion stability at narrow wire widths and the trapping of skyrmions at branching points in branch (hub) circuits, as shown in Fig. 3 (c). We therefore attempted to confine skyrmions within a channel by partially depositing an additional SiO₂ layer onto a continuous magnetic multilayer film. With this method, skyrmions were confirmed to appear and exhibit Brownian motion only in the regions without SiO₂, as shown in Fig. 3 (b). In other words, this method of partially depositing an additional SiO₂ layer enables the formation of a skyrmion circuit in the same manner as the method of forming magnetic wires by etching. This is attributed to a change in potential felt by the skyrmions, caused by a change in the magnetic properties of the underlying magnetic layer due to the partially deposited SiO₂ on the continuous film. Although strain in the magnetic layer is considered a possible origin of this change, it has not been confirmed in detail. However, unlike with the method using magnetic wires, it was shown that when the hub circuit shown in Fig. 3 (d) is formed by an additional SiO₂ layer, skyrmions exhibit smooth Brownian motion without being trapped at the branching points. This is because, in the method using the additional layer, strong pinning does not occur due to the non-uniform dipolar magnetic fields that arise when forming magnetic wires. From the above results, it can be concluded that skyrmion circuits that do not hinder Brownian motion can be formed when fabricating devices using skyrmions by employing a method in which a thin film is partially deposited onto a continuous film.



5. Fabricating cellular automaton devices using skyrmions

We fabricated a skyrmion device modeled after a quantum-dot cellular automaton to be used as an information device utilizing the above-mentioned method of partially depositing an additional SiO_2 layer onto a continuous film. A quantum-dot cellular automaton is a device that uses square-shaped cells with quantum dots placed at the four corners. When two electrons are confined within the quantum dots of these cells, the Coulomb repulsion force between the electrons causes them to occupy diagonally opposite positions to maximize their separation. As a result, the two most stable arrangements are the one with electrons at the top right and bottom left, and the other with electrons at the top left and bottom right. By defining the arrangements of quantum dots occupied by electrons as binary “0” and “1” as shown in Fig. 1 (c), the quantum-dot cellular automaton represents bits. In addition, by arranging multiple cells, it becomes possible to transmit information not only within individual cells but also between cells⁹. It was our aim to fabricate a skyrmion cellular automaton device based on this quantum-dot cellular automaton. As shown in Fig. 4, microfabrication on the surface of the



magnetic multilayer film where skyrmions appear caused a region with additional square-shaped SiO_2 layers to form. In Fig. 4 (b), l , d , and Δt represent the side length of the square, the distance between squares, and the thickness of the additionally deposited SiO_2 layer, respectively. Fig. 5 shows the magnetic structures observed using the MOKE microscope, with the size l of the additionally deposited square-shaped regions shown in Fig. 4 ranging from 3.1 to 10.3 μm . Measurements were conducted at room temperature (295 K), in air, and at an external vertical magnetic field of 0.25 mT. Skyrmions with diameters of 1 to 2 μm appeared in the regions with additionally deposited SiO_2 patterned layers, with the number of skyrmions appearing within each square increasing as l increased. In other words, by fabricating appropriately sized squares, it is possible to control the quantity of skyrmions. In cellular automaton-based calculations, it is necessary for two skyrmions to be confined within the squares, making 6.2 μm appropriate for l under the current conditions. It was found that keeping additional film thickness Δt at 0.5 nm or less enabled cell formation without creating any magnetic domains inside or outside the square-shaped region⁹. Fig. 6 (b) shows a MOKE microscope image of a device with l at 6.2 μm , d at 3.1 μm , and Δt at 0.2 nm. As can be seen in the figure, a pair of skyrmions is confined within each cell, and the device is expected to function as a skyrmion cellular automaton. In this experiment, skyrmions were generated in the parts with additionally deposited patterned layers, unlike the experiments shown in Fig. 3 (b) and (d). This is because the appearance of the skyrmion phase is not solely due to the effects of additional deposition on the magnetic film, but also depends on factors such as the degree of perpendicular magnetic anisotropy in the Co-Fe-B layer and the measurement temperature. Depending on the sample fabrication and measurement conditions, the skyrmion phase may also stabilize in the additionally deposited layers. Fig. 6 (c) plots the time-dependent y -positions of the skyrmions in Brownian motion nearest to the gap and confined in the left and right cells. The red plots indicate the y -positions of the skyrmion nearest to the gap in

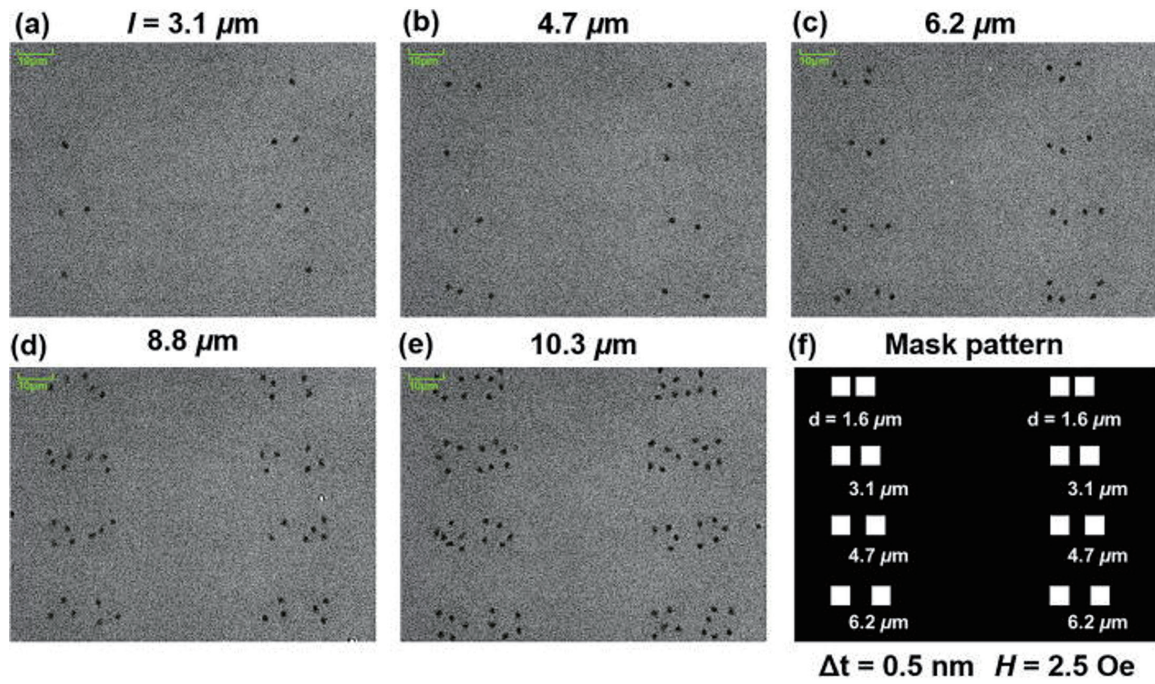


Fig. 5 Square size (l) dependence of a magnetic structure. The thickness of the additional SiO_2 (Δt) and the external magnetic field were fixed at 0.5 nm and 0.25 mT, respectively.

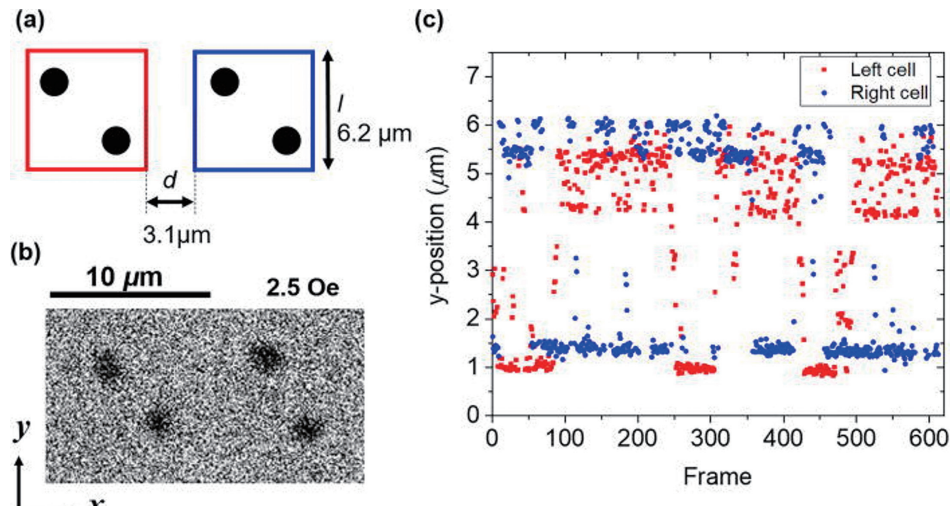


Fig. 6 (a) Schematic of designed dimension. (b) MOKE microscope image of two neighboring squares confining two skyrmions. (c) Time-dependent y -position of the two gap-side skyrmions confined in the left (red) and right (blue) cells.

the left square, while the blue plots indicate the skyrmion nearest to the gap in the right square. The graph shows behavior in which the y -positions appear to swap, such as how the skyrmion in the right square moves downward when the skyrmion in the left square moves upward. Calculating the correlation coefficient between

the two coordinates yields a value of -0.23 , clearly revealing a negative correlation. This result suggests that it may be possible to transmit information through the repulsive interaction between skyrmions in the left and right squares. To verify the possibility of zero-energy information processing using skyrmions in Brownian

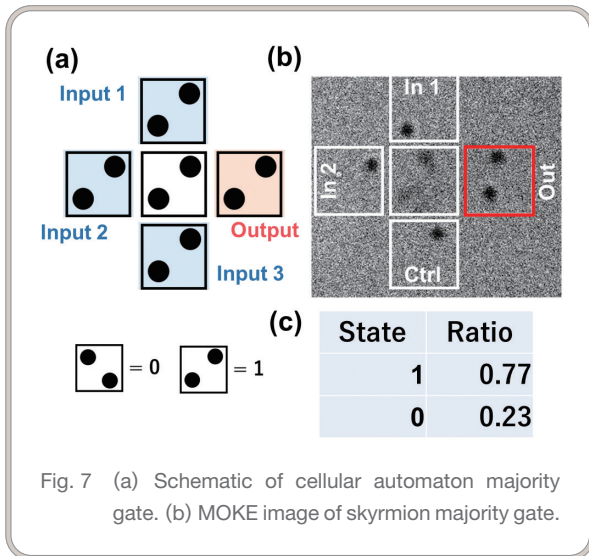


Fig. 7 (a) Schematic of cellular automaton majority gate. (b) MOKE image of skyrmion majority gate.

motion, a device was fabricated (Fig. 7 (b)) to mimic the majority gate proposed in quantum-dot cellular automata (Fig. 7 (a)). The three “Input” sections of the fabricated device use square regions of approximately the same size as the skyrmions, which prevents Brownian motion and causes them to function as fixed inputs. The central cell and “Output” section on the right are formed using the same $6.2\ \mu\text{m}$ square regions as in Fig. 6 (a). Because all three “Inputs” are set to “1” in this device, the correct result is for “Output” to also be “1”. In fact, by determining the state

at each moment on the basis of the relative positions of the two skyrmions in the “Output” section, the “1” state accounted for 77% of the total time, suggesting that the correct result can be obtained probabilistically. The above two experiments show that skyrmion cellular automata utilizing Brownian motion behave stochastically, unlike conventional cellular automata, suggesting their potential application in probabilistic computing.

6. Generation and annihilation of skyrmions by external voltage, and position control via interaction between skyrmions

Although it has been shown that the Brownian motion of skyrmions can be used for transmitting information and computing, external information input methods remain indispensable for applications in probabilistic computing and ultra-low-power computing. In this study, we therefore investigated whether skyrmions generated using voltage could be used to influence the positions of external skyrmions in Brownian motion. The device structure is shown in Fig. 8 (a) and (b). The structure consists of the previously mentioned multilayer film in which the skyrmions appear sandwiched between Ru electrodes, with the circuit section used to confine the skyrmions covered with $0.2\ \text{nm}$ of ultra-thin Pt. Using this structure makes it possible to observe the area directly beneath with a MOKE microscope while applying

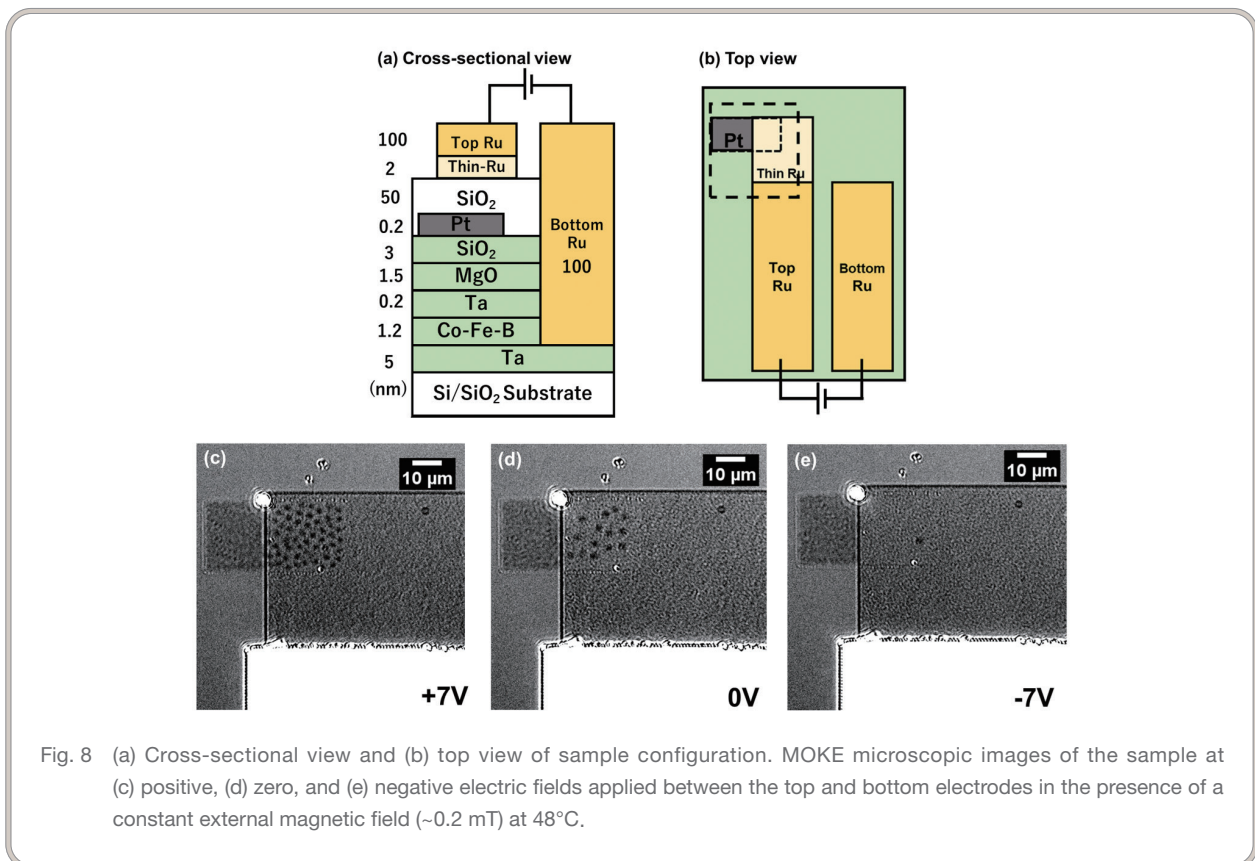


Fig. 8 (a) Cross-sectional view and (b) top view of sample configuration. MOKE microscopic images of the sample at (c) positive, (d) zero, and (e) negative electric fields applied between the top and bottom electrodes in the presence of a constant external magnetic field ($\sim 0.2\ \text{mT}$) at 48°C .

voltage. Fig. 8 (c), (d) and (e) show MOKE microscope images of the device when voltage is applied under an external magnetic field of approximately 0.2 mT. A change in voltage from positive to negative caused an observed decrease in skyrmion density. This change is thought to be due to altered skyrmion phase stability caused by modulation of perpendicular magnetic anisotropy by voltage. We next verified whether the positions of other skyrmions can be controlled by using the generation and annihilation of skyrmions by voltage. For this purpose, a device with narrower electrodes was fabricated, as shown in Fig. 9 (a). Fig. 9 (b) shows the MOKE microscope image when skyrmions appeared in the electrode-free region by applying an external magnetic field

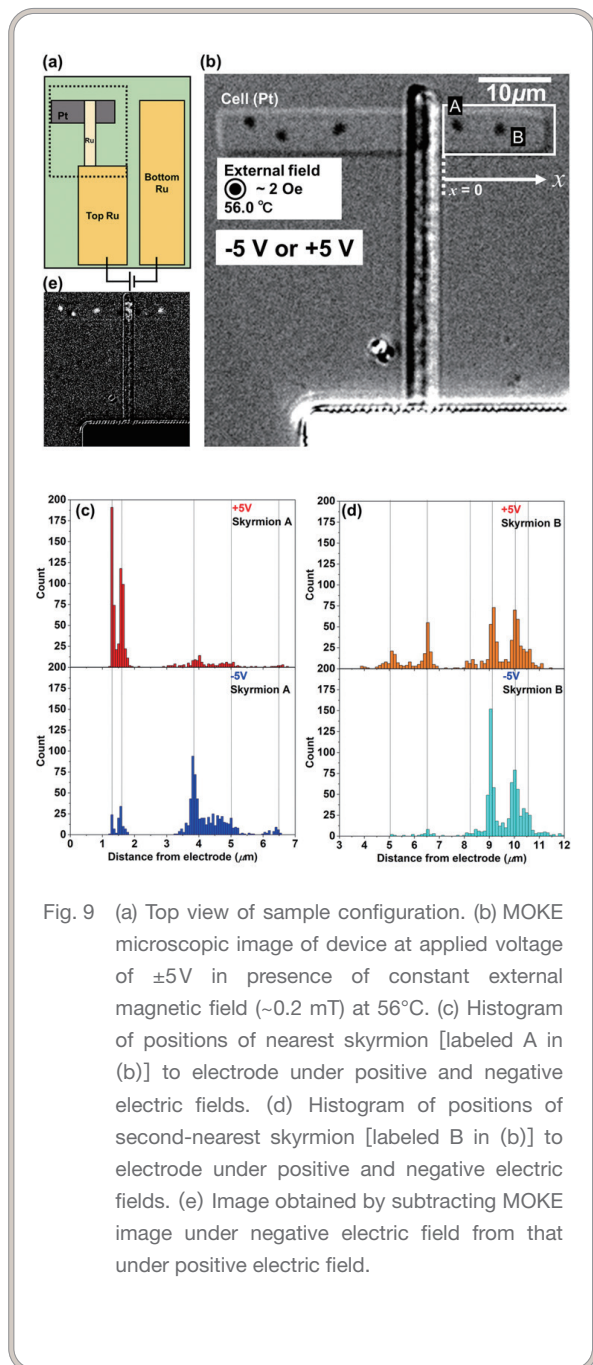


Fig. 9 (a) Top view of sample configuration. (b) MOKE microscopic image of device at applied voltage of ± 5 V in presence of constant external magnetic field (~ 0.2 mT) at 56°C . (c) Histogram of positions of nearest skyrmion [labeled A in (b)] to electrode under positive and negative electric fields. (d) Histogram of positions of second-nearest skyrmion [labeled B in (b)] to electrode under positive and negative electric fields. (e) Image obtained by subtracting MOKE image under negative electric field from that under positive electric field.

to the fabricated device. This experiment focused on the two skyrmions located in the region on the right-hand side of the electrode in the confined circuit (indicated by the white square in Fig. 9 (b)). The positions of the skyrmions were examined by observing the Brownian motion of the skyrmions for 25 seconds on two occasions, when $+5$ V and -5 V were applied to the device. Fig. 9 (c) and (d) are histograms that plot the positions occupied by the skyrmions with the right edge of the electrode as $x = 0$. When $+5$ V is applied, the average position of skyrmion A, which is closer to the electrode, is $2.4 \mu\text{m}$ from the electrode. On the other hand, when a voltage of -5 V is applied, the average position shifts to $4.0 \mu\text{m}$. This difference in distance is thought to be due to the repulsive magnetic dipole interaction between the skyrmions in the region without electrodes and those skyrmions generated beneath the electrode when a voltage of -5 V is applied. In fact, subtracting the MOKE microscope image under $+5$ V from the MOKE microscope image under -5 V yields the result shown in Fig. 9 (e), showing that when a negative voltage is applied, a region with the same magnetization orientation as the skyrmions in the vicinity is formed. This result demonstrates that the positions of skyrmions in Brownian motion outside the electrode can be changed by using the voltage-generated skyrmions via magnetic dipole interactions.

7. Controlling skyrmions by using a graded electric field

We will now introduce a study aimed at controlling skyrmions by using electrodes arranged in the in-plane direction by forming a gradient in magnetic anisotropy as a method for external skyrmion manipulation. Although changes in the velocity of domain wall motion under a sloped magnetic potential have already been investigated¹⁰⁾, the behavior of skyrmions in Brownian motion under a sloped potential has not yet been studied. Fig. 10 (a) and (b) show the device structure used to create the sloped potential, with thick Ru electrodes placed at both ends of an ultra-thin Ru electrode. Fig. 10 (c) and (d) show MOKE microscope images of the magnetic structure beneath the ultra-thin Ru electrode, with 0 V and 10 V applied to the signal (S) side in Fig. 10 (b). The figure shows that the width of the maze-like domain wall gradually changes between terminals when voltage is applied. To enable this change in domain wall width to be visualized, each image was sliced longitudinally and the number of domain walls was counted. It is anticipated that the wider the domain wall, the smaller the number of domain walls. Fig. 10 (e) shows the position dependence of the number of domain walls along the horizontal direction of the image, while the lines in the figure represent linear fits of the number of domain walls at each voltage. As the voltage increases, the number of domain walls decreases, indicating that the domain wall width increases from the ground side to the signal side. It was revealed that—because the width of the domain wall widens as the strength of the perpendicular magnetic anisotropy

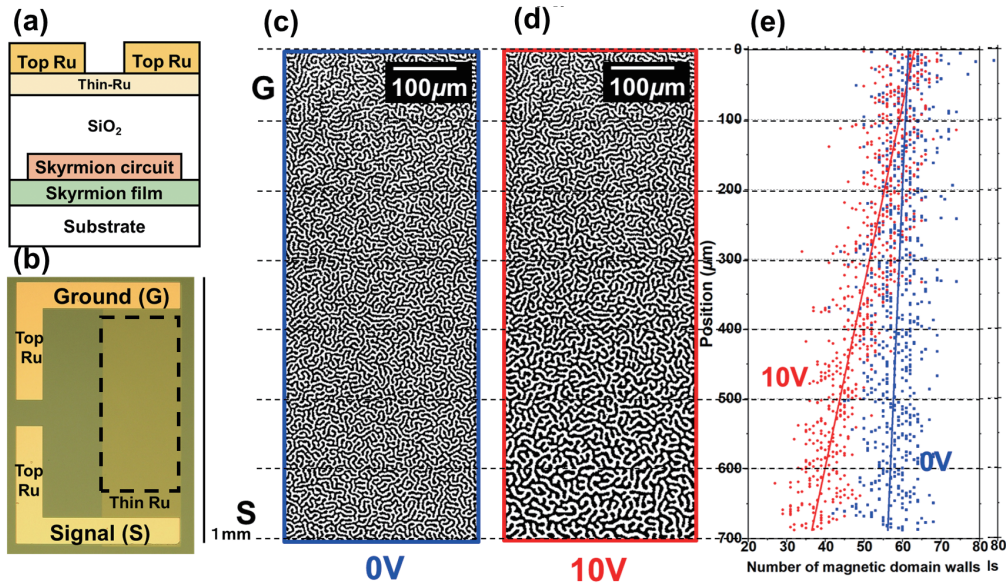


Fig. 10 (a) Cross-sectional and (b) top view of sample configuration. (c), (d) MOKE microscope observation by applying (c) 0 V and (d) +10 V between signal and ground electrode shown in (b). (e) Position dependence of the numbers of magnetic domain walls in (c) and (d).

increases—the perpendicular magnetic anisotropy is enhanced when a positive voltage is applied in the perpendicular direction in the fabricated device. Additionally, this gradual change in domain wall width indicates that a vertically graded voltage has been successfully formed. Fig. 11 shows the change in skyrmion distribution under a sloped potential. Compared to the moment at which voltage was first applied, skyrmions were observed to gradually move from the lower side to the upper side of the image over time. This is thought to be due to sloped voltage creating a gradient in the perpendicular magnetic anisotropy, which not only shifts the region where skyrmions stably exist but also causes skyrmions to move in Brownian motion along the gradient of the perpendicular magnetic anisotropy. This method can be applied to represent information based on the position and arrangement of the skyrmions in Fig. 1.

8. Summary

This study presented a method of controlling skyrmions for new computing principles based on skyrmions in Brownian motion, such as probabilistic computing and ultra-low-power computing. By developing skyrmion circuits and voltage control methods, a foundation is being formed for utilizing the thermally driven probabilistic behavior of skyrmions in new forms of computing. In the future, it will be necessary to fabricate information devices using the methods introduced here in order to evaluate the energy efficiency and probabilistic computing capabilities enabled by Brownian motion.

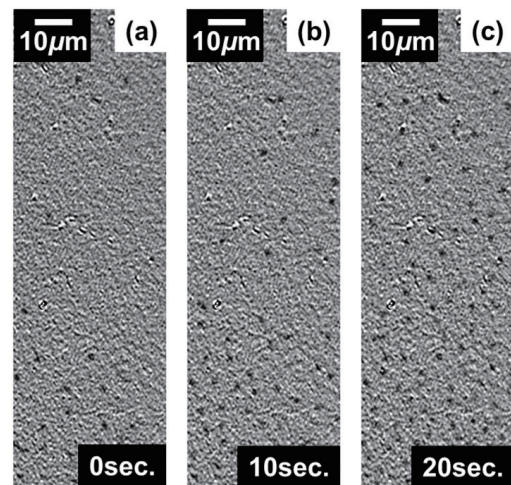
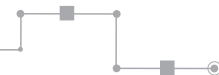


Fig. 11 MOKE image showing the change in distribution of skyrmions. (a) Initial state. (b), (c) After applying voltage for 10 or 20 seconds.

References

- 1) T. H. R. Skyrme: Nucl. Phys., **31**, 556 (1962).
- 2) U. K. Rößler, A. N. Bogdanov, and C. Pfleiderer: Nature, **442**, 797 (2006).
- 3) A. Fert, V. Cros, and J. Sampaio: Nat. Nanotechnol., **8** (3), 152 (2013).



- 4) X. Zhang, M. Ezawa, and Y. Zhou: *Sci. Rep.*, **5**, 9400 (2015).
- 5) J. Zázvorka, F. Jakobs, D. Heinze, N. Keil, S. Kromin, S. Jaiswal, K. Litzius, G. Jakob, P. Virnau, D. Pinna, K. Everschor-Sitte, L. Rózsa, A. Donges, U. Nowak, and M. Kläui: *Nat. Nanotechnol.*, **14**, 658 (2019).
- 6) T. Nozaki, Y. Jibiki, M. Goto, E. Tamura, T. Nozaki, H. Kubota, A. Fukushima, S. Yuasa, and Y. Suzuki: *Appl. Phys. Lett.*, **114**, 012402 (2019).
- 7) L. Zhao, Z. Wang, X. Zhang, X. Liang, J. Xia, K. Wu, H.-A. Zhou, Y. Dong, G. Yu, K. L. Wang, X. Liu, Y. Zhou, and W. Jiang: *Phys. Rev. Lett.*, **125**, 027206 (2020).
- 8) Y. Jibiki, M. Goto, E. Tamura, J. Cho, S. Miki, R. Ishikawa, H. Nomura, T. Srivastava, W. Lim, S. Auffret, C. Baraduc, H. Bea, and Y. Suzuki: *Appl. Phys. Lett.*, **117**, 082402 (2020).
- 9) C. S. Lent, P. D. Tougaw, W. Porod, and G. H. Bernstein: *Nanotechnol.*, **4**, 49 (1993).
- 10) H. Kakizakai, K. Yamada, F. Ando, M. Kawaguchi, T. Koyama, S. Kim, T. Moriyama, D. Chiba, and T. Ono: *Jpn. J. Appl. Phys.*, **56**, 050305 (2017).

[Acknowledgments]

We would like to thank the following (titles omitted): Eiiti Tamura, Yuma Jibiki, Yuji Tanaka, Yu Horiuchi, Ken Hashimoto, Hiroki Mori, Kota Emoto, Hiroto Imanishi, and Akifumi Shimmura of the Graduate School of Engineering Science, The University of Osaka; Chaozhe Liu of the Graduate School of Engineering, The University of Osaka; and Tenta Tani of the Graduate School of Science, The University of Osaka. We would also like to thank: Ferdinand Peper (theory) of the National Institute of Information and Communications Technology; Yasuhiro Utsumi and Yasuchika Ito (theory) of the Mie University Graduate School of Engineering; Takayuki Nozaki (MR measurements) of the National Institute of Advanced Industrial Science and Technology; Mikihiko Oogane (FMR measurements) of the Tohoku University Graduate School of Engineering; Yoichi Shiota (sputtering deposition) of the Kyoto University Institute for Chemical Research; and Chun-Yeol You and Jaehun Cho (BLS measurements) of DGIST.